BMC Cancer

RESEARCH

Open Access

RNF157 targets RIG-I/DDX58 to promote proliferation in liver cancer

Changsong Ma[1], Qingsong Yang[1], Gaoyuan Yu[3], Ao Li[1], Congyin Tu[2], Jian Wang[2], Wei Zhang[1], Lin Chen[2], Da Teng[1], Qinweng Wang[1], Yongjun Shao[2], Yang Zhang[2] and Wengjun Zhang[1*]

Abstract

Liver cancer is one of the most common malignant tumours in humans, and a large proportion of patients are diagnosed at an advanced stage due to rapid growth and distant metastasis; thus, there is an urgent need to identify critical genes involved in the development of liver cancer. In this study, we investigated the role of RING finger protein 157 (RNF157) in liver cancer proliferation and the related mechanisms. First, we used bioinformatics counting for database mining of RNF157 expression in hepatocellular carcinoma and paracancerous tissues and its relationship with prognosis. We detected the expression level of RNF157 in human samples and different liver cancer cell lines via fluorescence quantitative polymerase chain reaction (Q-PCR), Western blot, and immunohistochemistry (IHC). Subsequently, virus transfection was used to construct knockdown and overexpressed stably transfected cell lines to test the effect of RNF157 on the proliferation of liver cancer. Immunoprecipitation (Co-IP) was used to verify the binding and regulatory relationship between RNF157 and RIG-I/DDX58. We found that RNF157 expression was significantly upregulated in liver cancer tissues and correlated with poor prognosis. In addition, knockdown of RNF157 expression inhibited liver cancer cell proliferation and overexpression of RNF157 promoted liver cancer cell proliferation. Co-IP results revealed that RNF157 binds to and downregulates the expression level of RIG-I/DDX58, further suggesting that RNF157 binds to and ubiquitinates RIG-I/DDX58 at residue 48 of the lysine, which leads to a significant increase in the expression level of RIG-I/DDX58. In this study, we found that RNF157 is a tumour-promoting ubiquitin ligase that promotes liver cancer growth by targeting RIG-I/DDX58 for degradation. Thus, RNF157 has the potential to be a therapeutic target for liver cancer.

Keywords Ubiquitination, E3 ubiquitin ligases, RNF157, RIG-I/DDX58, Hepatocellular carcinoma

Introduction

Liver cancer is one of the most prevalent malignant tumours in China, and hepatocellular carcinoma (HCC) is the most common type of liver cancer, accounting for approximately 90% of all liver cancer cases [1]. Due to the difficulty of early diagnosis of liver cancer and the lack of characteristic tests, it is difficult to detect liver cancer early, resulting in high mortality [2]. In recent years, an increasing number of new biological markers have been used for the diagnosis of early-stage liver cancer, such as alpha-fetoprotein heterodimer (AFP-L3) [3], abnormal plasminogen (DCP) [4], phosphatidylinositol proteoglycan-3 (GPC3) [5], and Golgi apparatus-73 (GP73)

*Correspondence:
Wengjun Zhang
zwj821373223@163.com
[1] Hepatobiliary Surgery, Affiliated Chuzhou Hospital of Anhui Medical University, First People's Hospital of Chuzhou, No.369 Zuiweng West Road, Nanqiao District, Chuzhou 239000, China
[2] Department of Hepatobiliary Surgery, Division of Life Sciences and Medicine, The First Affiliated Hospital of USTC, University of Science and Technology of China, Hefei 230001, China
[3] Department of Thyroid and Breast Surgery, Anhui Provincial Hospital Affiliated With Anhui Medical University, Hefei 230001, China

[6], but all of these markers lack specificity and sensitivity. Therefore, exploring the mechanism of liver cancer development and discovering new diagnostic and therapeutic targets are highly important for the treatment of this disease.

Ubiquitin (Ub) is a highly conserved 76-amino-acid protein in eukaryotes. As one of the most prevalent post-translational modifiers of proteins, Ub binds to lysine residues of a wide range of cellular proteins and plays an important role in regulating cellular functions [7]. The process of ubiquitination is catalysed sequentially by three enzymes, including E1Ub-activating enzyme, E2Ub-binding enzyme and E3Ub protein ligase [8]. Dysfunction of the protein ubiquitination system is closely associated with the generation and development of various tumours, such as breast cancer [9]. Ring finger protein 157 (RNF157) belongs to the ring finger protein family, has E3 ubiquitin ligase activity, and is involved in a variety of cellular regulatory activities. Studies [10] have shown that RNF157 promotes neuronal cell survival and is a key regulator. Moreover, RNF157 can play an important role in tumour proliferation by regulating the cell cycle and differentiation [11, 12]. For example, exosome-mediated RNF157 mRNA in prostate cancer cells promotes prostate tumour progression by disrupting the stability of HDAC1 and leading to the polarization of M2 macrophages [13]. RIG-I/DDX58 is a member of the RIG-I-like receptor (RLR) family, and its activity can be regulated by a variety of E3 ubiquitinases, which play important roles in tumour progression. However, the roles of RNF157 in liver tumours have rarely been reported; therefore, this study aimed to investigate the biological function and potential mechanism of action of RNF157 in liver cancer. Our study revealed that RNF157 expression is significantly upregulated in liver cancer tissues and is associated with poor prognosis. In addition, knocking down RNF157 expression can inhibit the proliferation of liver cancer cells and, conversely, promote the proliferation of liver cancer cells. Furthermore, RNF157 was found to incorporate the ubiquitination of RIG-I/DDX58 at lysine 48, resulting in RIG-I/DDX58 degradation to promote liver cancer cell proliferation.

Materials and methods

Cell culture and transfection

The liver tumour cell lines Huh-7, Hep-G2, HCCLM3, Hep-3B and SUN-387 were all imported from Wuhan Punocai Life Technology Co., Ltd. All of them were authenticated by STR profiling, and they were supplemented with 10% foetal bovine serum (FBS), streptomycin (100 IU/mL), penicillin (100 μg/mL), and improved Eagle medium (DMEM; HyClone) for Huh-7, Hep-G2, and HCCLM3 cells. RPMI-I640 (1640; HyClone) was used for the Hep-3B and SUN-387 cell lines. The cells were cultured in a constant-temperature humidified incubator at 37 °C with 5% CO_2. The RNF157-overexpressing cell line was constructed via virus transfection of Huh-7 cells, and the RNF157-knockdown cell line was constructed via virus transfection of HCCLM3 and Hep-3B cells. The plasmid used for overexpression of RNF157: Homo sapiens ring finger protein 157 (RNF157), transcript variant 1, mRNA NCBI Reference Sequence: NM_052916.3. The over-expressed control virus is an empty control virus without inserting foreign genes. RNF157 was knocked down by lentivirus and transfected into tumor cells. The sequence of the virus used for RNF157 knockdown was RNF157 shRNA-1:GGATCCCATCCATCCTCAGAGAATATTTTCAAGAGAAATATTCTCTGAGGATGGATGTTTTTTGAATTC; RNF157 shRNA-2:GGATCCGGGTAGCCATCACCATCTATTTTCAAGAGAAATAGATGGTGATGGCTACCCTTTTTTGAATTC; negative control: GGATCCACTACCGTTGTTATAGGTGTTCAAGAGACACCTATAACAACGGTAGTTTTTTTGAATTC. Two thousand cells were cultivated in a 6-well plate, the virus and transfection reagents (Lipofectamine 8000, Beyotime, C0533) were added, and the medium was changed 8 h later. After 48 h, puromycin (5 μg/ml) was added, and the cells were incubated for 72 h. After the untreated group was completely killed with puromycin, the medium was replaced with complete culture medium, the medium was expanded, and the cells were frozen for later use. The transfection efficiency was evaluated via quantitative real-time polymerase chain reaction (q-PCR) and Western blot.

Clinical tissue samples

All samples were from patients who underwent hepatectomy in Chuzhou First People's Hospital from December 2023 to March 2024, and the postoperative pathology was confirmed as liver cancer. Six of the 8 patients were HBV positive, all of whom were treated with antiviral drugs, and 2 patients who were HBV negative had different drinking histories. All patients were diagnosed with liver cancer for the first time and had not received any treatment (surgery, locoregional, systemic). The experiment was approved by the Chuzhou first people's hospital medical ethics Committee (2023) Lun Shen 【Biology】 No. (2).

Immunohistochemistry

The tissue microarray (TMA) was purchased from Shanghai Xinultra Biotechnology Co., Ltd. The tissue samples were fixed with 4% paraformaldehyde, dehydrated with gradient alcohol, treated with xylene transparently, hydrated with gradient alcohol, repaired with

antigens, inactivated with endogenous enzymes, sealed with sealing solution, placed in an anti-wetting box at 4 °C overnight, incubated with secondary antibodies at room temperature for 30 min, incubated with mycobiotin-hydrogen peroxide solution at room temperature for 10 min, washed and subjected to DAB staining.

Total protein extraction and Western blot detection

The cell suspension was collected and cleaved with RIPA (32010A, Bebo Bio, Inc.) lysis buffer containing a protease inhibitor. After centrifugation, the supernatant was harvested, and the protein concentration was measured via the BCA method. An appropriate amount of 2×loading buffer (1,610,737, BIO RAD) was added, after which the mixture was denatured in a water bath and cooled on ice. The protein was separated by electrophoresis on a 10% sodium dodecyl sulfate–polyacrylamide gel and then transferred to a PVDF membrane. After the samples were blocked with 5% skim milk, RNF157 primary antibody (YT6295, Immunoway Company), RIG-I/DDX58 primary antibody (3B10F5, Proteintech), GAPDH (AB0037, Shanghai Bowan Biotechnology Co., Ltd.), HA-RNF157 (51,064–2-AP, Proteintech), Myc-DDX58 (60,003–2-Ig, Proteintech), and Ub-Flag (20543–1-AP, Proteintech) were incubated at 4 °C overnight. The membranes were then incubated with a horseradish peroxidase-coupled secondary antibody (AB0102, Shanghai Bowan Biotechnology Co., Ltd.) at room temperature for 1 h. The protein bands were visualized via an enhanced chemiluminescence kit (Beyotime, Shanghai), and the relative grey values were calculated via ImageJ software.

Total RNA extraction and real-time polymerase chain reaction (q-PCR) detection

The cell suspension was placed in RNA lysis buffer (RNA lysis buffer:β-oleophobic ethanol = 1000:20), and the total RNA was reverse-transcribed into complementary DNA (cDNA) according to the SYBR fluorescent real-time PCR kit. The analysis was carried out by Applied Biosystems (USA), and the cycle conditions were 37 °C for 15 min, 85 °C for 15 s, and cooling to 4 °C for 10 min. Each reaction was repeated 3 times. The mRNA expression was analysed by the $2^{-\Delta\Delta Ct}$ method, and glyceraldehyde 3-phosphate dehydrogenase (GAPDH) was used as the reference gene. The sequences of primers used in this assay were as follows: RNF157-F: GGCTTTGATTTAGACCGAGAA; RNF157-R: CTTCGTCTTCAGCCACCTTA; GAPDH-F:GAGAAGTATGACAACAGCCTCAA; GAPDH-R: GCCATCACGCCACAGTTT.

CCK-8 experiment

The exponentially grown Huh-7, HCCLM3, Hep-3B cells (100 μL, 1×10^4 cells/mL) were inoculated into 96-well plates. The samples were incubated with 5% CO_2 at 37 °C overnight, 5 μL of CCK-8 (C0038, Beyotime) was added to each well at 24, 48, 72, 96, and 120 h, the samples were incubated at 37 °C for 2 h, and the absorbance at 450 nm was measured via a spectrophotometer.

Plate cloning experiment

Huh-7, HCCLM3, Hep-3B cells were inoculated into 6-well plates ($1*10^3$ cells/well), 2 mL of complete culture medium was added, and the cells were cultured in a humidified incubator at 37 °C and 5% CO_2. The culture medium was changed every 4 days, the cells were fixed with 4% paraformaldehyde after 10 days, stained with crystal violet, and photographed under an optical microscope, and the experimental results were analysed via ImageJ software.

Subcutaneous tumorigenesis in nude mice

Five-week-old athymic BALB/c nude mice were purchased from Hangzhou Ziyuan Experimental Animal Science and Technology Co., Ltd., and housed in SPF class animal housing. Hep-G2 does not carry the genome of the hepatitis B virus, and it does not cause tumors in immunosuppressed mice. Therefore, we chose the HCCLM3 and Hep-3B cells, which have a faster tumor growth rate. Isoflurane inhalation anesthesia, use an induction concentration of 3–5% with an oxygen flow rate of 1–2 L/min for rapid induction. After achieving anesthesia, reduce the concentration to 1–2% with an oxygen flow rate of 0.5–1 L/min for maintenance. Adjust the anesthetic concentration in real-time based on respiratory rate and responses to toe pinch reflex while continuously monitoring body temperature and other vital parameters to ensure the safety of the mice. A total of 3×10^6 /200ul control cells and RNF157-overexpressing Huh7/knockdown HCCLM3 and Hep-3B hepatoma cells were injected subcutaneously into the groin of nude mice, There were 5 participants in the experimental group and 5 participants in the control group. We observe the health of the laboratory animals every day, The tumour volume was measured each week, After about 4 weeks, the tumors were isolated for analysis. The tumor volume.

was calculated as Length × Width × Width × 0.5. It is generally recommended that the tumor volume should not exceed 10% of the body weight of the mice. The tumor volume should be controlled below 1500 mm^3.All mice were euthanized using cervical dislocation. Confirmed cervical dislocation with respiratory and cardiac arrest. Because cervical dislocation is a physical method, it is usually combined with pupillary reflex examination to ensure death. The subcutaneous tumours were weighed, and a tumour growth curve was drawn. All animal experiments were undertaken and conducted with

approval from the ethics review committee of Chuzhou First People's Hospital.

Coimmunoprecipitation (Co-IP)

HCCLM3 and Hep-3B cells were lysed with RIPA buffer, and the supernatant was incubated with primary antibodies against RNF157 and RIG-I/DDX58 at 4 °C overnight; 5% was used as the input lysate, and the remaining mixture was incubated at 4 °C with protein A/G magnetic beads. For exogenous immunoprecipitation, the cell lysate was incubated with Myc beads (MedChemExpress) and HA beads (MedChemExpress) overnight, centrifuged and washed with IP lysis buffer three times, and the protein expression level was detected via Western blotting.

RNA sequencing

To explore the potential mechanism of RNF157 in liver cancer, RNA sequencing was performed. A lentivirus was used to construct stable RNF157 cells from Huh-7 cells, and the overexpression efficiency was verified via q−PCR. The cells in the control group and RNF157 overexpression group were sent to Shanghai Oui Biomedical Technology Co., Ltd., for RNA-Seq detection. Sequencing of the library produced a paired-end reading of 150 bp (TruSeq Stranded mRNA LTSample Prep Kit, Illumina, RS-122–2101; Agencourt AMPure XP, BECKMAN COULTER, A63881; Qubit RNA Assay Kit, Life Technologies, Q32852; Qubit dsDNA Assay Kit, Life Technologies, Q328520; Bioanalyzer 2100 RNA-6000 Nano Kit, Agilent, 5067–1511; Bioanalyzer 2100 DNA-1000 Kit Agilent, 5067–1504; SuperScript II Reverse Transcriptase, Invitrogen, 18,064,014) on an Illumina HiSeq X Ten platform (cat. no. DOE20221816; Illumina, Inc.). An Agilent 2100 bioanalyzer was used to measure the length and quality of the library. The Phred score determines the base error rate in Illumina sequencing and is calculated by the model to predict the probability of errors in base differentiation. Raw data in fastq format (raw readings) are first processed via Trimmomatic (version 0.36), and low-quality readings are removed for clean reading. Subsequently, approximately 14,000 clean readings of each sample were retained for analysis. Clean readings were plotted onto the human genome (GRCh38) via HISAT2 (version 2.2.1.0). Cufflinks (version 2.2.1) was used to calculate the number of transcription fragments per kilobase per million map readings for each gene, and the reading for each gene was obtained via HTSeq count (version 0.9.1). The concentration of RNA samples can be quickly measured via a NanoDrop spectrophotometer, and the purity of RNA can be assessed by the absorption rate (A260/A280 and A260/A230). An A260/A280 ratio close to 2.0 usually indicates less protein contamination, whereas an A260/A230 ratio greater than 2.0 indicates less contamination from organic solvents or other impurities. The DESeq (version 1.18.0) R software package was used for differential expression analysis. $P < 0.05$ and FC > 1.5 or < 0.5 were set as thresholds for significant differential expression. Systematic cluster analysis of DEGs was performed to demonstrate the expression patterns of genes in different groups and samples. Based on hypergeometric distribution, gene ontology (http://geneontology.org) enrichment analysis of DEGs and KEGG enrichment analysis were performed via R (version 4.3.3, integrated R archive network). The data are available via the Sequence ReadArchive identifier PRJNA1107826.

Proteomic sequencing

To explore the potential mechanism of RNF157 in liver cancer, proteomic sequencing was performed. A lentivirus was used to construct stable RNF157 Huh-7 cells, and the overexpression efficiency was detected by Western blotting. The cells were then sent to Hangzhou Jingjie Biotechnology Co., Ltd., for proteomic detection. ProteomeXchange dataset has been made public via the PRIDE database (http://www.ebi.ac.uk/pride/archive/projects/PXD052805).

Immunofluorescence

The ordinary clean cover glass was placed in a 24-well plate, HCCLM3 cells ($2*10^4$ cells/mL) were inoculated and incubated with 5% CO_2 at 37 °C overnight so that the cell density was approximately 50%, the culture medium was removed, the mixture was washed twice with 1 ml of PBS, 1 ml of paraformaldehyde was added, the mixture was fixed at room temperature for 15 min, and the mixture was sealed with sealing liquid (1 ml/well) for 60 min. RNF157 and RIG-I/DDX58 antibodies were added to 0.5 ml/well diluted fluorescent secondary antibodies overnight at 4 °C and incubated at room temperature for 40 min in the dark. The samples were then incubated with DAPI (50 μl/well) for 5 min in the dark and observed via fluorescence microscopy.

Statistical analysis

The results are expressed as the mean ± standard deviation or the standard error of the mean and were analysed with GraphPad Prism 8 software. After the normality of the raw data was tested, Student's t test was used to analyse the differences between two independent groups. One-way analysis of variance (ANOVA) was used to determine the differences between groups. $p < 0.05$ was considered statistically significant.

Results

RNF157 is overexpressed in liver cancer

We first analysed RNF157 expression in liver cancer in the TCGA database. Publicly available data revealed that RNF157 was significantly elevated in liver cancer tissue compared with normal liver tissue (Fig. 1A). To confirm this finding, we collected 8 pairs of clinical liver cancer and paracarcinoma tissue samples and examined protein expression levels in these tissues via Western blot analysis, as well as protein blotting to detect protein expression in different liver cancer cell lines, including Huh-7, Hep-G2, HCCLM3, Hep-3B, and SUN-387, and Q-PCR, to detect mRNA expression levels. These experiments revealed elevated expression levels of RNF157 protein and corresponding mRNA in liver cancer (Fig. 1B, C, D), and further analysis revealed that RNF157 expression was relatively high in Hep-G2, HCCLM3, and Hep-3B cells and relatively low in Huh-7 cells. Immunohistochemical staining of microarrays containing cancer and adjacent samples from 75 liver cancer patients revealed that high expression of RNF157 was detected in multiple stages of liver cancer (Fig. 1E).

High expression of RNF157 is significantly associated with poor prognosis in liver cancer

The TCGA database also revealed that the expression of RNF157 is different in liver cancer with different degrees of differentiation and stages. The expression of RNF157 is greater in poorly differentiated or undifferentiated liver cancer, suggesting that RNF157 may be related to the progression of liver cancer rather than the number of lymph node metastases in patients. There was a significant difference in RNF157 expression among patients with different TP53 mutation statuses ($P<0.001$) (Fig. 2A). K–M analysis revealed that the RNF157 expression level in liver cancer is related to overall survival (OS), progression-free survival (PFS), and recurrence-free survival (RFS); that is, patients with high RNF157 expression have poorer outcomes, suggesting that high RNF157 expression is significantly associated with poor prognosis in cancer patients (Fig. 2B). Interestingly, a survival follow-up of 29 patients treated with sorafenib revealed that patients with different RNF157 expression levels did not have the same survival time with sorafenib treatment, although the difference was not statistically significant ($P=0.058$). However, it is worthwhile to explore the possibility of following more patients, as the results suggest that patients with high RNF157 expression levels may be more resistant to sorafenib, which provides a good opportunity for clinical sorafenib treatment for liver cancer patients and provides a potential strategy. The expression of different RNF157 levels is more clinically relevant in Asian populations than in Caucasian populations, suggesting that low RNF157 levels may be a protective factor in Asians (Fig. 2C).

Knockdown of RNF157 inhibits liver cancer proliferation

In HCCLM3 and Hep-3B cells, we used lentivirus transfection to construct a stably transfected cell line in which RNF157 was knocked down and used Western blotting to detect the knockdown efficiency (Fig. 3A). CCK-8 and plate cloning experiments were subsequently performed. Compared with the control, shRNF157 inhibited the proliferation of liver cancer cells (Fig. 3B, C). In xenograft mouse models, the inhibition of RNF157 significantly slowed the growth of subcutaneous tumours in mice. Compared with that in the control group, the average tumour weight was lower in the shRNF157 group (Fig. 3D).

Overexpression of RNF157 promotes liver cancer proliferation

The corresponding lentivirus was used to construct control and RNF157-overexpressing Huh-7 cells. The overexpression efficiency was detected via Western blot analysis (Fig. 4A). CCK-8 and plate colony formation assays revealed that, compared with that in the control group, liver cancer cell proliferation was greater in the RNF157-OE group (Fig. 4C, D). Compared with those in the control group, the tumours in the RNF157-OE group were faster. In addition, the RNF157-OE group had greater tumour weights compared with the other groups (Fig. 4E). These results indicate that RNF157 can promote the proliferation of liver cancer cells in vitro and in vivo. The KEGG functional enrichment results of proteome sequencing revealed that RNF157 may be involved in extracellular matrix receptor interactions and signalling pathways such as the Wnt and HIF-1 pathways (Fig. 4B).

RNF157 interacts with RIG-I/DDX58

To study the potential mechanism, RNF157-overexpressing stably transfected Huh-7 cells were generated, and the control group and Huh-7-OE histone proteins were sequenced. RNF157 overexpression downregulated the protein expression level of RIG-I/DDX58. Subsequent immunofluorescence localization experiments revealed that the binding of RNF157 and RIG-I/DDX58 was located in the nucleus (Fig. 5D). For further coimmunoprecipitation experiments, anti-RNF157, RIG-I/DDX58 and IgG antibodies were used to coimmunoprecipitate HCCLM3 and Hep-3B cell lysates, and Western blot analysis was used to detect the endogenous interaction between RNF157 and RIG-I/DDX58. RNF157 and RIG-I/DDX58 plasmids were cotransfected into HEK293T cells, which were then cultured for 48 h. The cells were

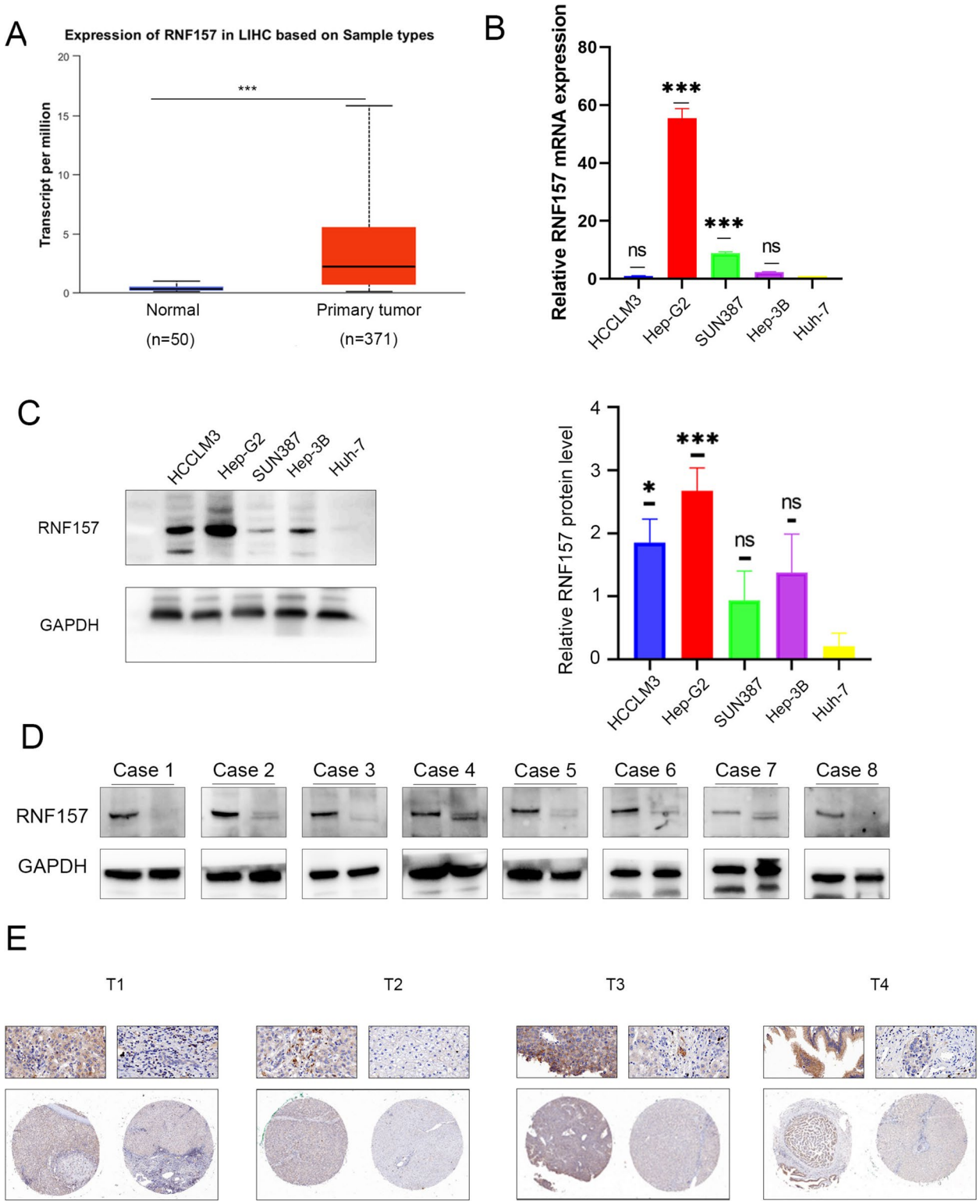

Fig. 1 RNF157 expression in liver tumour tissues and cell lines (**A**) RNF157 expression in liver cancer and normal liver tissues with data from the TCGA database. **B** mRNA levels of RNF157 in Huh-7, Hep-G2, HCCLM3, Hep-3B, and SUN-387 cells analysed by q–PCR. **C** RNF157 expression in Huh-7, Hep-G2, HCCLM3, Hep-3B, and SUN-387 cells was detected via protein blot analysis. **D** Protein levels of RNF157 in 8 pairs of liver cancer and neighbouring normal liver tissues were analysed by protein blotting. **E** Microarray immunohistochemical staining of RNF157 in liver cancer and neighbouring normal tissues ($n = 75$). * indicates $P < 0.05$, ** indicates $P < 0.01$, *** indicates $P < 0.001$

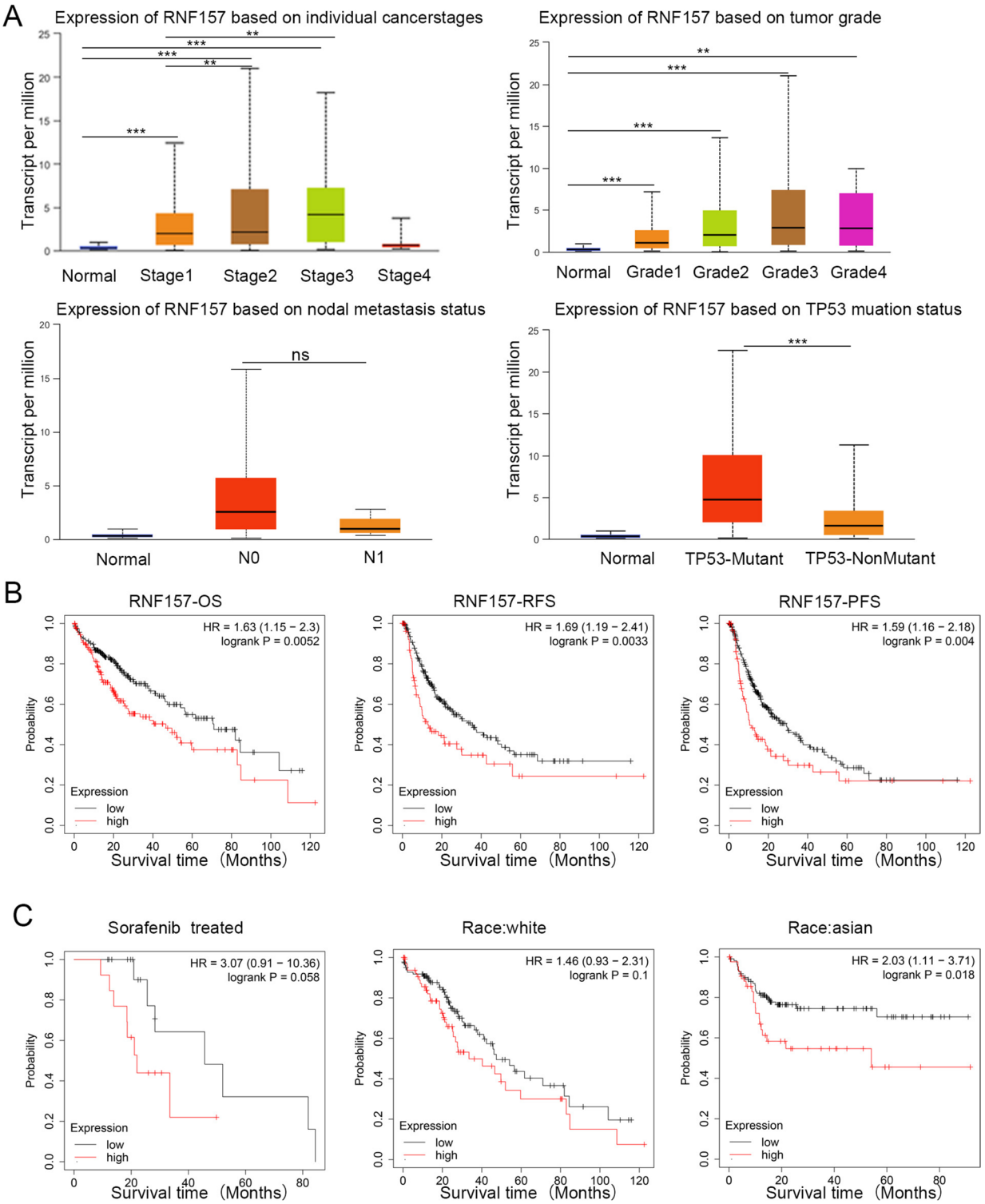

Fig. 2 Relationships between RNF157 expression and clinical prognosis in the TCGA database. **A** Relationships between RNF157 RNA levels and different stages, grades, degrees of lymph node metastasis, and TP53 mutation types. **B** Kaplan–Meier evaluation of the relationships between RNF157 expression and overall survival (OS), relapse-free survival (RFS), and progression-free survival (PFS) rates. **C** Survival curves of patients with different expression levels of RNF157 after sorafenib treatment; survival curves of Caucasians and Asians with different expression levels of RNF157. ns indicates no significant difference, * indicates $P < 0.05$, ** indicates $P < 0.01$, and *** indicates $P < 0.001$

treated with MG132 6 h before lysis and then immunoprecipitated with anti-HA or anti-Myc magnetic beads. Western blot analysis was performed with anti-HA or anti-Myc antibodies. Regarding the exogenous interaction between RNF157 and RIG-I/DDX58, the results revealed that RNF157 and RIG-I/DDX58 bind to each other in HCCLM3, Hep-3B and HEK293T cells (Fig. 5A, B, C).

RNF157 regulates RIG-I/DDX58 stability in a ubiquitination-dependent manner

To clarify the regulatory effect of RNF157 on RIG-I/DDX58, we used anti-RNF157 and anti-RIG-I/DDX58 antibodies to perform Western blot detection in HCCLM3-knockdown, Hep-3B-overexpressing and Huh-7-overexpressing cells. We found that the RNF157 level was negatively correlated with the RIG-I/DDX58 ratio. Specifically, knockdown of RNF157 can cause an increase in RIG-I/DDX58, whereas overexpression of RNF157 can cause a decrease in RIG-I/DDX58 (Fig. 6A). After gradient transfection of HEK293T cells with different concentrations of the RNF157 plasmid, we also found that the level of RIG-I/DDX58 decreased as the concentration of RNF157 increased (Fig. 6B). To further study the effect of RNF157 on the ubiquitination of the RIG-I/DDX58 protein, we transiently cotransfected the RNF157, RIG-I/DDX58 and Ub WT, Ub K48, and Ub K63 plasmids into HEK293T cells. After being cultured for 48 h, the cells were treated with MG132 for 6 h before lysis. An anti-Myc magnetic bead antibody was used for coimmunoprecipitation, and an anti-HA antibody, anti-Myc antibody and anti-Flag antibody were used for Western blot analysis and detection. RNF157 promoted the overall polyubiquitination and lysine 48 (K48)-linked ubiquitination of RIG-I/DDX58 in HEK293T cells but did not change the lysine 63 (K63)-linked ubiquitination of RIG-I/DDX58 (Fig. 6C).

Discussion

Although the pathogenesis of liver cancer is still poorly understood, the posttranslational modification of proteins is considered an important factor in liver cancer pathogenesis. The UPS is the most important pathway for protein degradation in eukaryotic cells and is involved in important physiological and biochemical processes, such as cell growth, differentiation, DNA replication and repair, cell metabolism, and the immune response. There is increasing evidence that dysregulation of cycloubiquitin protein ligase (E3), which acts as a tumour promoter or suppressor in liver cancer under specific conditions, is associated with the development of liver cancer. RNF157, which has E3 ubiquitin ligase activity, plays important roles not only in neuronal regulation but also in the occurrence and development of ovarian epithelial cancer, thyroid cancer, oral squamous cell cancer and other tumours [14–16]. It has also been reported to regulate CD4+T-cell-mediated autoimmune responses [17]. Although the potential role of RNF157 in a variety of diseases, especially tumours, has gradually been discovered, there is currently a lack of research on its role in liver cancer. A prognostic study based on a TCGA cohort consisting of 11 RNFPS genes (RNF220, RNF25, TRIM25, BMI1, RNF216P1, RNF115, RNF2, TRAIP, RNF157, RNF145, and RNF19B) revealed that RNFF-related gene profiles could be used to evaluate liver cancer prognostic indices [18] to guide the treatment of liver cancer, but a detailed exploration of specific genes is lacking. In this study, we found that RNF157 is highly expressed in liver cancer and is closely related to prognosis at the tissue and cell levels. The ubiquitin ligase E3 also plays an important role in the tumour signal transduction pathway. RNF43 and ZNRF3 are known negative regulators of the Wnt pathway. By targeting the Wnt receptor Frizzled, it induces ubiquitination-mediated lysosomal degradation to control Wnt signal transduction, thus controlling the activation of the Wnt signal transduction pathway [19]. RNF157 is involved in the activation of multiple pathways and is the "connecting point" of the MAPK/ERK and PI3K/AKT signalling pathways, among which the ERK pathway is one of the classical pathways related to the regulation of cell proliferation [20]. In the overexpression group (OE) compared to the normal control group (NC), the top 20 significant pathways were identified through statistical enrichment analysis. Our RNA-seq analysis results revealed that RNF157 is related to Wnt signalling, HIF-1 signalling, and ECM-receptor

(See figure on next page.)

Fig. 3 RNF157 knockdown inhibits liver cancer cell proliferation. **A** After lentiviral transfection, Western blot analysis of RNF157 knockdown efficiency in HCCLM3 and Hep-3B cells was performed. **B** Proliferation levels of HCCLM3 and Hep-3B cells were assessed via a CCK-8 assay. **C** A plate cloning experiment was performed to detect the proliferation of HCCLM3 and Hep-3B cells. **D** Images of tumours removed from nude mice four weeks after subcutaneous injection of HCCLM3 and Hep-3B cells ($n=5$). The tumour weights of the two groups of nude mice were measured. Tumour diameter was used to plot tumour volume curves. The images are from one representative experiment, and the data are expressed as the means ± SDs of three independent experiments (*$p<0.05$, **$p<0.01$, ***$p<0.001$). Ordinary one-way ANOVA with multiple comparisons testing was used to examine the statistical significance of differences among the three independent groups

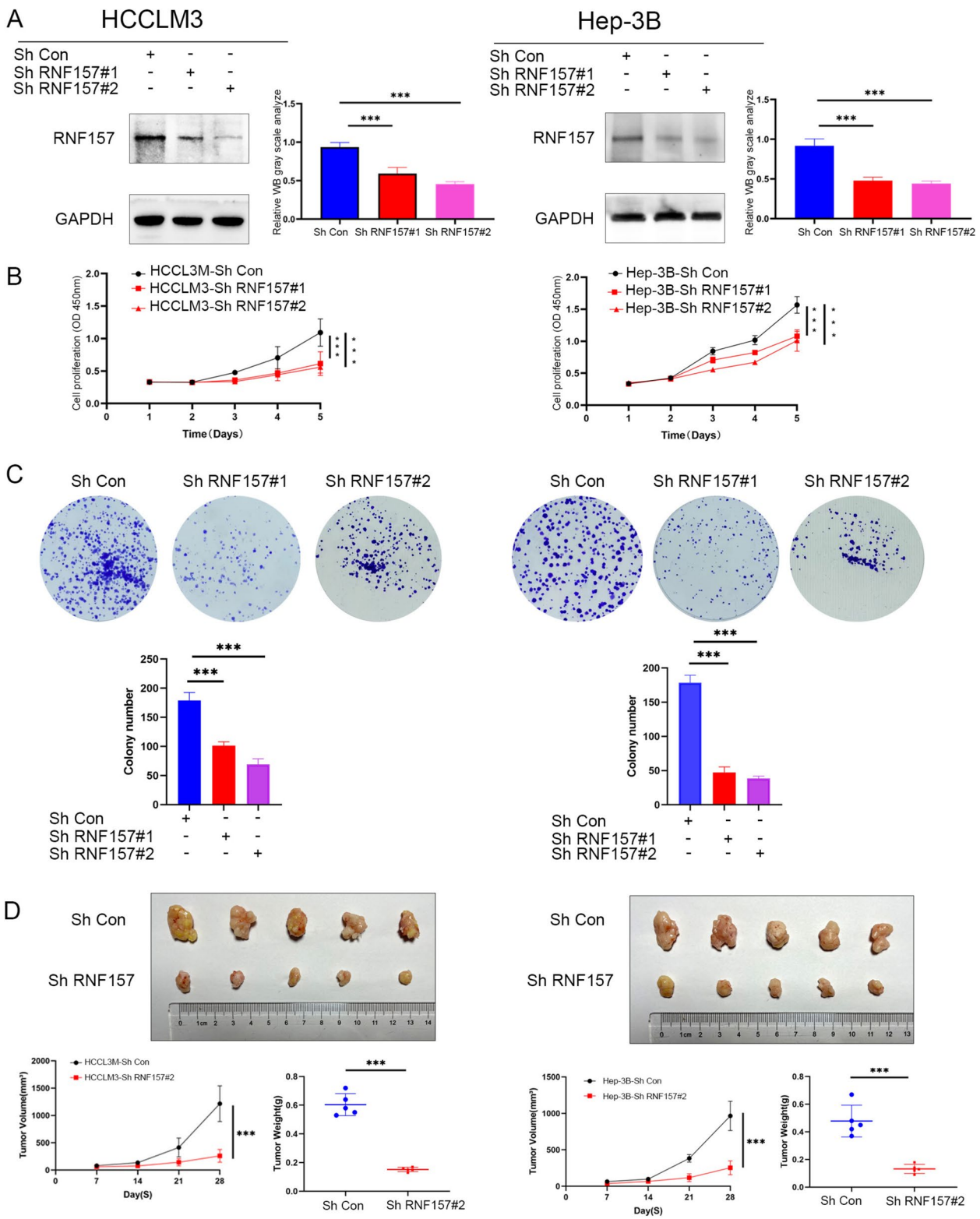

Fig. 3 (See legend on previous page.)

interactions,The study revealed that "RNF157"may play a potential role in cancer-related pathways, metabolic pathways, and immune/inflammatory-related pathways. The inhibition of "basal cell carcinoma"and "proteoglycan pathways"suggests possible activation of specific tumor suppression mechanisms or disruption of tumor-related signaling by the overexpressed gene. The downregulation of metabolic pathways likely reflects weakened cellular energy metabolism (e.g., glycolysis) and impaired amino acid metabolism in the OE group. Reduced functionality of the "complement system", "B cells", and "NK cells" may compromise immune surveillance capacity, thereby promoting tumor immune escape.

RIG-I, also known as DDX58, is a member of the RIG-I-like receptor (RLR) family with RNA helicase activity (including DEX/DH boxes) [21], which plays an important role in viral infection. It can recognize viral double-stranded RNA (dsRNA) to produce type I interferons (IFN-a and IFN-b) to exert antiviral effects [22]. Among hepatitis B viruses, novel coronavirus infections related to neurological diseases are crucial [23, 24]. In addition, RIGI was found to be significantly reduced in a mouse model of nonalcoholic steatohepatitis (NASH), while its stable overexpression protects cells from palmitic acid toxicity and stimulates autophagy. Therefore, the activation of RIG-I-induced autophagy may be a treatment method for nonalcoholic fatty liver disease (NAFLD) [25]. In recent years, RIG-I has been recognized as a pattern recognition receptor that recognizes nucleic acids released by dead and damaged cancer cells. Moreover, immune cells such as dendritic cells (DCs), CD8 + T cells and natural killer (NK) cells are recruited into the tumour microenvironment to kill tumour cells [26, 27]. Another function of RIG-I is to exert antitumour effects by binding to a variety of transcription factors; for example, RIG-I regulates the STAT3/CSE signalling pathway by interacting with STAT3, thus affecting the proliferation of colon cancer tumour cells [28]. The activity of RIG-I can be enhanced by E3 ubiquitination enzymes such as TRIM25 via K63-linked ubiquitination, thus promoting the activation of downstream RIG-I signalling [29]. Moreover, CD97 inhibits the antiviral response by upregulating RNF125 expression and inducing RIG-I degradation through Lys181 ubiquitination linked to K48 [30]. With the in-depth study of immune checkpoint inhibitors, the treatment options for liver cancer are becoming increasingly diverse; the recent treatment approach for the systemic treatment of liver cancer is based on the combination of immune checkpoint inhibitors plus tyrosine kinase inhibitors to enhance the anticancer immune response and block tumour cell proliferation and neoangiogenesis, as described in a recent comprehensive review [31]. In this study, via protein interaction screening, we identified the E3 ubiquitin ligase RNF157 as a novel protein that interacts with RIG-I. RNF157 promotes the ubiquitination of RIG-I at the lysine 48 residue and causes its degradation. This finding suggests that RNF157 may be a negative regulator of RIG-I at the posttranscriptional level. The downregulation of RIG-I/DDX58 by RNF157 may affect the cell cycle in liver cancer occurrence and development through a DNA damage repair mechanism, providing ideas for further research. Interestingly, patients with high levels of RNF157 expression may be more resistant to sorafenib, Although there was no statistical significance at present, there may be different results with the increase of sample size, which provides a potential target for genetic testing and clinically targeted immunotherapy for liver cancer. This may be particularly relevant in Asian populations with low expression of RNF157. Considering the difference of RNF157 expression in different populations and demographics, studying these factors can help to develop more targeted treatment methods. Clinical trials can stratify participants according to demographic factors to obtain more accurate data about the effect of RNF157 targeted therapy in different populations. In addition, the screening of RNF157 level in specific high-risk population may be helpful for early intervention, thus improving the prognosis. Understanding the role of RNF157 in different cancers and diseases from the perspective of population and demographic differences may ultimately help to improve the individualization of treatment and provide a valuable direction for further research.

However, as a preliminary study, this study has several limitations. Although this study suggested that RNF157 promotes liver cancer proliferation by targeting RIG-I/

(See figure on next page.)

Fig. 4 RNF157 overexpression promotes CC cell proliferation. **A** Western blotting and detection of RNF157 expression in Huh7 cells after transfection of the overexpression sequence. **B** OE-control protein sequencing KEGG functional enrichment. **C** CCK-8 assay was used to assess the proliferation level of Huh7 cells. **D** A plate colony formation assay was performed to detect the proliferation level of Huh7 cells. **E** Images of tumours removed from nude mice four weeks after the subcutaneous injection of Huh-7 cells ($n = 5$). The tumour weights of the two groups of nude mice were measured. Tumour diameter was used to plot tumour volume curves. The images are from one representative experiment. The data are expressed as the means ± SDs of three independent experiments (*$p < 0.05$, **$p < 0.01$, ***$p < 0.001$). Ordinary one-way ANOVA with multiple comparisons testing was used to examine the statistical significance of differences among the three independent groups

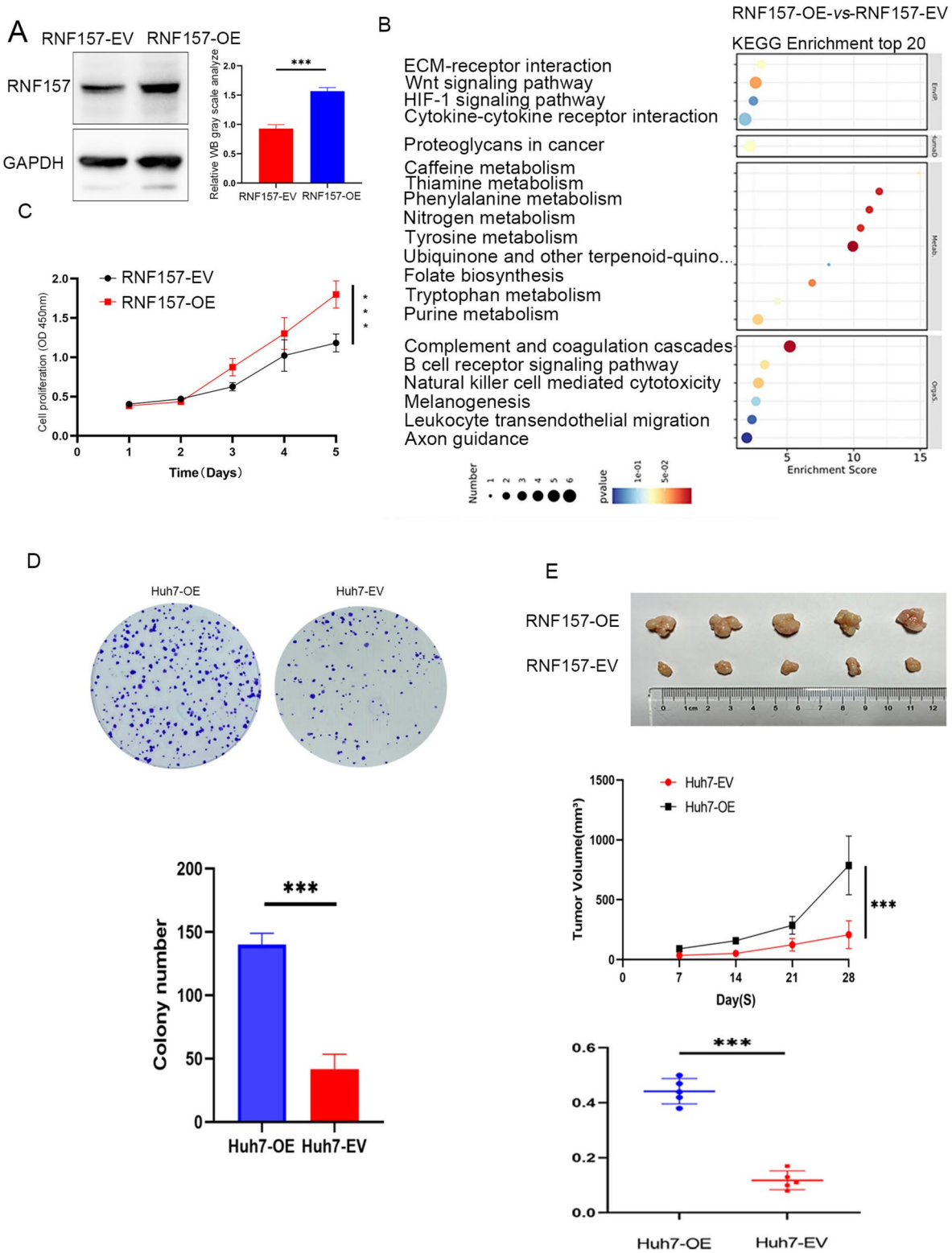

Fig. 4 (See legend on previous page.)

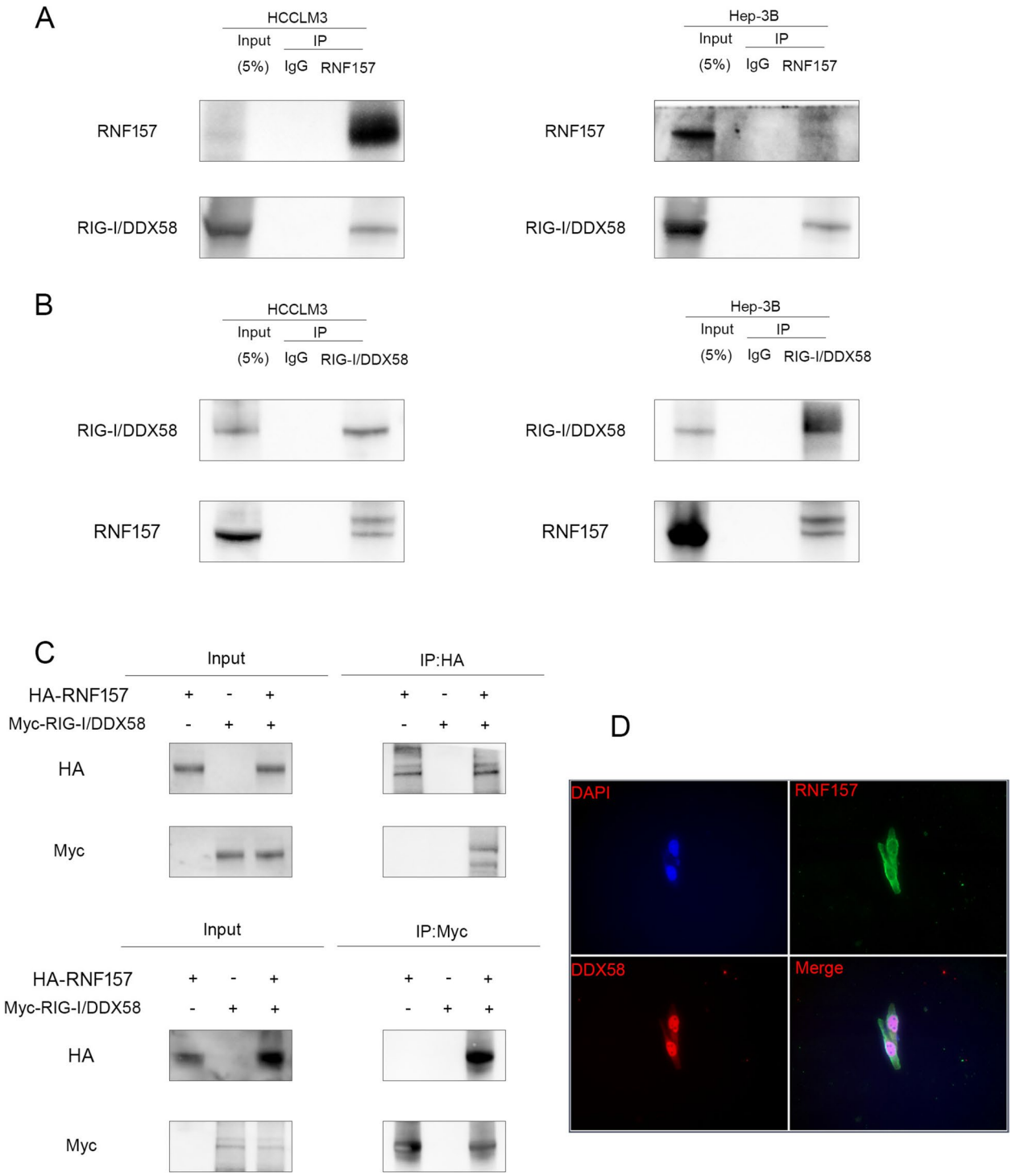

Fig. 5 RNF157 binds to DDX58. Anti-RNF157, anti-DDX58, and IgG antibodies were used to coimmunoprecipitate HCCLM3 and Hep-3B cell lysates, and Western blot analysis was performed to detect the endogenous interaction between RNF157 and DDX58 (Fig. 5 **A**, **B**). Lysates from HEK293T cells cotransfected with HA-RNF157 or Myc-DDX58 were treated, immunoprecipitated with anti-HA or anti-Myc magnetic bead antibodies, and then subjected to Western blotting with anti-HA or anti-Myc antibodies, respectively (Fig. 5 **C**). Assays to detect exogenous interactions between RNF157 and DDX58 were performed. Immunofluorescence revealed the colocalization of RNF157 (green) and DDX58 (red) in HCCLM3 cells, and the nuclei were stained with DAPI (Fig. 5 **D**)

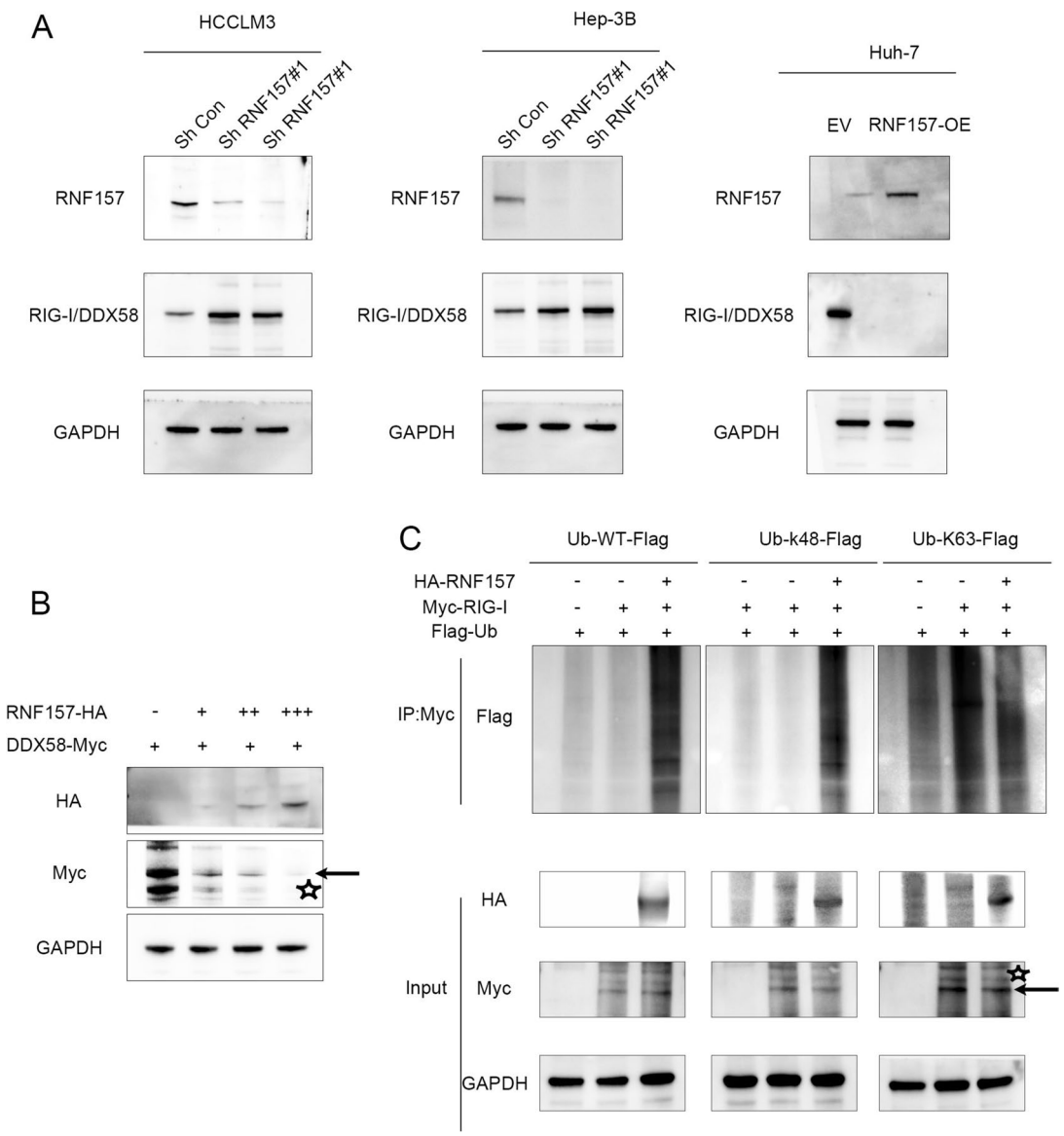

Fig. 6 RNF157 mediates K48 ubiquitination of DDX58. **A** HCCLM3 and Hep-3B cells were knocked down, Huh7 cells were overexpressed, and Western blot analysis was performed using RNF157 and DDX58 antibodies. Huh7-overexpressing cells were subjected to Western blot analysis with an RNF157 antibody and a DDX58 antibody. **B** HEK293T cells were cotransfected with different doses (0, 1, 2, or 4 μg) of HA-RNF157 and 4 μg of the Myc-DDX58 plasmid and cultured for 48 h. Western blot analysis was performed after treatment with MG132 (20 μM) for 6 h. **C** Lysates from HEK293T cells transiently cotransfected with Flag-Ub (K48, K63, KWT), HA-RNF157, or Myc-DDX58 were treated, immunoprecipitated with anti-Myc antibodies, and then treated with anti-HA, anti-Myc, or anti-Flag antibodies for Western blot analysis

DDX58, The relatively small sample size and overrepresentation of HBV-positive cases in this study may restrict the extrapolation of results to other etiologies (e.g., HCV, alcohol-related liver disease). Future large-scale, multi-etiology prospective studies are required to validate the universality of these findings. this study utilized hepatocellular carcinoma cell lines (including HCCLM3 and Hep-3B) that do not fully represent the heterogeneity of liver cancer subtypes. Additionally, the reliance on subcutaneous xenograft models in animal experiments represents a limited approach. To address these limitations, future studies will incorporate orthotopic implantation models and broader HCC subtype coverage to enhance the robustness of conclusions. Moreover, Immunofluorescence analysis revealed co-localization of RNF157 with RIG-I/DDX58 in the nucleus. Notably, while RIG-I/DDX58 is predominantly localized in the cytoplasm (where it mediates antiviral responses),

its nuclear localization observed here suggests potential involvement in transcriptional regulation or DNA damage repair-related mechanisms. Further studies are warranted to investigate the functional implications of this nuclear compartmentalization. Therefore, it is necessary to expand the sample size to improve the accuracy of the experiment. In the future research, We will construct a domain mutant of RNF157 protein to explore the structural region of the interaction between RNF157 and RIG-I/DDX58, make a protein half-life experiment to clarify the half-life of RIG-I/DDX58, and further explore the possible ways of degradation of RIG-I/DDX58, such as lysosomal dependence or autophagy.

Conclusion

In summary, we identified RNF157 as a tumour promoter in liver cancer. It can target RIG-I/DDX58 for proteasome-dependent degradation to promote liver cancer proliferation. Our study revealed that targeting RNF157 may be a potential treatment for liver cancer.

Supplementary Information

The online version contains supplementary material available at https://doi.org/10.1186/s12885-025-14224-7.

Supplementary Material 1.

Acknowledgements
Not applicable.

Patient consent for publication
Not applicable.

Authors' contributions
Concept and design: MCS, YQS, ZWJ. Experiment performance: MCS, LA, WJ, WQW, and LC. Data analysis and interpretation: MCS, YQS, ZY, ZW, and SYJ. Writing and review of the manuscript: MCS, LA, TD. Article revision: YYG, SY, TC. Supervision: ZWJ, YQS.

Funding
The experimental site of this study was provided by Chuzhou First People's Hospital and supported by the Anhui Provincial Clinical Medical Research Transformation Project (202204295107020062) and the Anhui Medical University Research Fund project (2023xkj094).

Data availability
Sequence data that support the findings of this study have been deposited in the European Nucleotide Archive with the primary accession code PRJNA1107826. The mass spectrometry proteomics data have been deposited to the ProteomeXchange Consortium via the PRIDE partner repository with the dataset identifier PXD052805.reviewer can access the dataset by logging in to the PRIDE website using the following account details: Username: reviewer_pxd052805@ebi.ac.uk ; Password: 5ikM0TITa0Nr. Alternatively, The data can be accessed directly through the following websites. (https://proteomecentral.proteomexchange.org/cgi/GetDataset?ID=PXD052805).

Declarations

Ethics approval and consent to participate
Liver tumour tissue samples were obtained from patients treated at Chuzhou First People's Hospital, and written informed consent was obtained. All experiments were approved by the Medical Ethics Committee of Chuzhou First People's Hospital (approval number (2023) Lun Shen 【Biology】 No. (2)) and our study adhered to the Declaration of Helsinki.

Competing interests
The authors declare no competing interests.

Received: 2 November 2024 Accepted: 24 April 2025
Published online: 01 May 2025

References

1. Vogel A, Meyer T, Sapisochin G, Salem R, Saborowski A. Hepatocellular carcinoma. Lancet. 2022;400:1345–62. https://doi.org/10.1016/S0140-6736(22)01200-4.
2. Wang W, Wei C. Advances in the early diagnosis of hepatocellular carcinoma. Genes Dis. 2020;7:308–19. https://doi.org/10.1016/j.gendis.2020.01.014.
3. Yi X, Yu S, Bao Y. Alpha-fetoprotein-L3 in hepatocellular carcinoma: a meta-analysis. Clin Chim Acta. 2013;425:212–20. https://doi.org/10.1016/j.cca.2013.08.005.
4. Chen H, et al. Direct comparison of five serum biomarkers in early diagnosis of hepatocellular carcinoma. Cancer Manag Res. 2018;10:1947–58. https://doi.org/10.2147/CMAR.S167036.
5. Zhou F, Shang W, Yu X, Tian J. Glypican-3: A promising biomarker for hepatocellular carcinoma diagnosis and treatment. Med Res Rev. 2018;38:741–67. https://doi.org/10.1002/med.21455.
6. Jiao C, Cui L, Piao J, Qi Y, Yu Z. Clinical significance and expression of serum Golgi protein 73 in primary hepatocellular carcinoma. J Cancer Res Ther. 2018;14:1239–44. https://doi.org/10.4103/0973-1482.199784.
7. Wang D, Bu F, & Zhang W. The Role of Ubiquitination in Regulating Embryonic Stem Cell Maintenance and Cancer Development. Int J Mol Sci. 2019;20. https://doi.org/10.3390/ijms20112667
8. Pickart CM. Mechanisms underlying ubiquitination. Annu Rev Biochem. 2001;70:503–33. https://doi.org/10.1146/annurev.biochem.70.1.503.
9. Howley BV, et al. The ubiquitin E3 ligase ARIH1 regulates hnRNP E1 protein stability EMT and breast cancer progression. Oncogene. 2022;41:1679–90. https://doi.org/10.1038/s41388-022-02199-9.
10. Matz A, et al. Regulation of neuronal survival and morphology by the E3 ubiquitin ligase RNF157. Cell Death Differ. 2015;22:626–42. https://doi.org/10.1038/cdd.2014.163.
11. Dogan T, et al. Role of the E3 ubiquitin ligase RNF157 as a novel downstream effector linking PI3K and MAPK signaling pathways to the cell cycle. J Biol Chem. 2017;292:14311–24. https://doi.org/10.1074/jbc.M117.792754.
12. Kosacka J, et al. Up-regulated autophagy: as a protective factor in adipose tissue of WOKW rats with metabolic syndrome. Diabetol Metab Syndr. 2018;10:13. https://doi.org/10.1186/s13098-018-0317-6.
13. Guan H, et al. Exosomal RNF157 mRNA from prostate cancer cells contributes to M2 macrophage polarization through destabilizing HDAC1. Front Oncol. 2022;12:1021270. https://doi.org/10.3389/fonc.2022.1021270.
14. Xu, P. et al. Differential effects of the LncRNA RNF157-AS1 on epithelial ovarian cancer cells through suppression of DIRAS3- and ULK1-mediated autophagy. Cell Death Dis. 2023;14. https://doi.org/10.1038/s41419-023-05668-5
15. Tian J, Luo B, Wang F. Identification of Three Prognosis-Related Differentially Expressed lncRNAs Driven by Copy Number Variation in Thyroid Cancer. J Immunol Res. 2022;2022:1–18. https://doi.org/10.1155/2022/9203796.
16. Lv S, et al. Identification and Validation of a Hypoxia-Immune-Based Prognostic mRNA Signature for Oral Squamous Cell Carcinoma. J Oncol. 2022;2022:1–16. https://doi.org/10.1155/2022/5286251.
17. Wang P, et al. RNF157 attenuates CD4+ T cell-mediated autoimmune response by promoting HDAC1 ubiquitination and degradation. Theranostics. 2023;13:3509–23. https://doi.org/10.7150/thno.86307.
18. Zhang C, et al. The Systematic Analyses of RING Finger Gene Signature for Predicting the Prognosis of Patients with Hepatocellular Carcinoma. J Oncol. 2022;2022:1–17. https://doi.org/10.1155/2022/2466006.

19. Farnhammer F, Colozza G, Kim J. RNF43 and ZNRF3 in Wnt Signaling - A Master Regulator at the Membrane. Int J Stem Cells. 2023;16:376–384. https://doi.org/10.15283/ijsc23070
20. Codenotti S, et al. Caveolin-1 enhances metastasis formation in a human model of embryonal rhabdomyosarcoma through Erk signaling cooperation. Cancer Letters. 2019;449:135–44. https://doi.org/10.1016/j.canlet.2019.02.013.
21. Wicherska-Pawłowska K, Wróbel T, & Rybka J. Toll-Like Receptors (TLRs), NOD-Like Receptors (NLRs), and RIG-I-Like Receptors (RLRs) in Innate Immunity. TLRs, NLRs, and RLRs Ligands as Immunotherapeutic Agents for Hematopoietic Diseases. Int J Mol Sci. 2021;22. https://doi.org/10.3390/ijms222413397
22. Onomoto K, Onoguchi K, Yoneyama M. Regulation of RIG-I-like receptor-mediated signaling: interaction between host and viral factors. Cell Mol Immunol. 2021;18:539–555. https://doi.org/10.1038/s41423-020-00602-7
23. Phillips S, Jagatia R, Chokshi S. Novel therapeutic strategies for chronic hepatitis B. Virulence. 2022;13:1111–32. https://doi.org/10.1080/21505594.2022.2093444.
24. Gugliandolo, A. et al. SARS-CoV-2 Infected Pediatric Cerebral Cortical Neurons: Transcriptomic Analysis and Potential Role of Toll-like Receptors in Pathogenesis. Int J Mol Sci. 2021;22. https://doi.org/10.3390/ijms22158059
25. Frietze KK, et al. Lipotoxicity reduces DDX58/Rig-1 expression and activity leading to impaired autophagy and cell death. Autophagy. 2021;18:142–60. https://doi.org/10.1080/15548627.2021.1920818.
26. Kanneganti T-D, Lamkanfi M, Núñez G. Intracellular NOD-like Receptors in Host Defense and Disease. Immunity. 2007;27:549–59. https://doi.org/10.1016/j.immuni.2007.10.002.
27. Iurescia S, Fioretti D. Rinaldi M. Targeting Cytosolic Nucleic Acid-Sensing Pathways for Cancer Immunotherapies. Front Immunol. 2018;9. https://doi.org/10.3389/fimmu.2018.00711
28. Deng Y. et al. Activation of DDX58/RIG-I suppresses the growth of tumor cells by inhibiting STAT3/CSE signaling in colon cancer. Int J Oncol. 2020;61. https://doi.org/10.3892/ijo.2022.5410
29. Gack MU, et al. TRIM25 RING-finger E3 ubiquitin ligase is essential for RIG-I-mediated antiviral activity. Nature. 2007;446:916–20. https://doi.org/10.1038/nature05732.
30. Chang H, et al. CD97 negatively regulates the innate immune response against RNA viruses by promoting RNF125-mediated RIG-I degradation. Cell Mol Immunol. 2023;20:1457–71. https://doi.org/10.1038/s41423-023-01103-z.
31. Stefanini B, et al. TKIs in combination with immunotherapy for hepatocellular carcinoma. Expert Rev Anticancer Ther. 2023;23:279–91. https://doi.org/10.1080/14737140.2023.2181162.

Publisher's Note